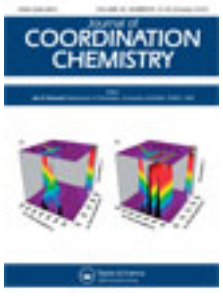

Journal of Coordination Chemistry
Publication details, including instructions for authors and subscription information:
http://www.tandfonline.com/loi/gcoo20

Syntheses, structures, and fluorescent properties of two helical complexes based on a long rigid N-heterocyclic ligand

Gang Han [a], Yajuan Mu [a], Dongqing Wu [a], Yanyuan Jia [a], Hongwei Hou [a] & Yaoting Fan [a]

[a] Department of Chemistry, Zhengzhou University, Zhengzhou, Henan 450052, P.R. China

Accepted author version posted online: 09 Aug 2012.Published online: 04 Sep 2012.

To cite this article: Gang Han, Yajuan Mu, Dongqing Wu, Yanyuan Jia, Hongwei Hou & Yaoting Fan (2012) Syntheses, structures, and fluorescent properties of two helical complexes based on a long rigid N-heterocyclic ligand, Journal of Coordination Chemistry, 65:20, 3570-3579, DOI: 10.1080/00958972.2012.719610

To link to this article: http://dx.doi.org/10.1080/00958972.2012.719610

Journal of Coordination Chemistry
Vol. 65, No. 20, 20 October 2012, 3570–3579

Syntheses, structures, and fluorescent properties of two helical complexes based on a long rigid N-heterocyclic ligand

GANG HAN, YAJUAN MU, DONGQING WU, YANYUAN JIA, HONGWEI HOU* and YAOTING FAN

Department of Chemistry, Zhengzhou University, Zhengzhou, Henan 450052, P.R. China

(*Received 14 January 2012; in final form 20 June 2012*)

A long N-heterocyclic ligand, 2,6-bis(3-(pyrid-3-yl)-1,2,4-triazolyl)pyridine (H_2bptp), and Zn(II)/Pb(II) yield $\{[Zn(bptp)(H_2O)]\cdot 2H_2O{\cdot}CH_3CN\}_n$ (**1**) and $\{[Pb(bptp)]\cdot H_2O\}_n$ (**2**). Single-crystal X-ray diffraction analysis reveals that **1** and **2** possess 2-D networks containing alternating left- and right-handed helical motifs. Topologically, **1** features a (4,4) topology, while **2** exhibits a (6,3) topology. The $bptp^{2-}$ in **1** and **2** adopts *syn-anti* and *syn-syn* conformations, respectively. The results indicate that the long rigid N-heterocyclic ligand can adopt different conformations to coordinate with metals, beneficial to construction of helical structures with diverse topologies. The difference between the photoluminescence properties of the two complexes reveals that metal ions and coordination environment have significant influences on photoluminescence behavior.

Keywords: Helical complexes; The steric effect; Photoluminescent properties; Long rigid N-heterocyclic ligand

1. Introduction

Helical complexes have attracted interest in coordination chemistry because of intriguing structures and potential applications in molecular recognition, nonlinear optical materials, asymmetric catalysis, enantiomorph separation, medicine, etc. [1]. Although helical structures have been reported [2], control of helices remains a challenge since the self-assembly process is complicated and frequently influenced by many factors [3]. More research is needed on relevant structural types and to establish the proper correlation between desired helical structures and optimized properties.

Rigid nitrogen heterocyclic ligands have been utilized as building blocks for the construction of helical structures [4]. For example, pyrazole linked bis(pyridine) gives $[\{Fe^{II}(\mu\text{-}L)_3\}_2Fe^{III}_3(\mu\text{-}O)]^{2+}$ (L = 3,5-bis(pyridin-2-yl)pyrazolate) with a pentanuclear M_5L_6 cluster helicate [5]. Two factors are important for self-assembly of helical complexes based on rigid nitrogen heterocyclic ligands. One is that nitrogen atoms of heterocyclic rings from branched chains of rigid ligands directly coordinate with metal ions [6]. The orientational freedom of lone pairs may be reduced using rigid backbones,

*Corresponding author. Email: houhongw@zzu.edu.cn

ISSN 0095-8972 print/ISSN 1029-0389 online
http://dx.doi.org/10.1080/00958972.2012.719610

helpful to terminal nitrogen atoms bound to metal centers. The second is that the ligands and the metal centers are not co-planar [7]. Long rigid ligands can rotate on account of the steric effect about the central C–C and C–N bonds [8]. Because of the rotation, heterocyclic ligands can adopt different conformations [9]. Complexes constructed by long rigid ligands may show complicated and interesting helical structures. Compared with complexes based on flexible and semi-rigid ligands, complexes produced from long rigid ligands present higher emission intensity because of the increase of the rigidity of organic rings [10].

We chose 2,6-bis(3-(pyrid-3-yl)-1,2,4-triazolyl)pyridine (H_2bptp), where geometry distortion can occur when central nitrogen atoms coordinate to metal in chelating mode. In this article, we present two new 2-D helical complexes based on H_2bptp, $\{[Zn(bptp)(H_2O)] \cdot 2H_2O \cdot CH_3CN\}_n$ (**1**) and $\{[Pb(bptp)] \cdot H_2O\}_n$ (**2**). The crystal structures and topological analyses of these two complexes will be discussed. In addition, the thermal stabilities and photoluminescence in the solid state have also been investigated.

2. Experimental

2.1. *Materials and physical techniques*

All reagents and solvents were obtained from commercial sources and used without purification. IR data were recorded on a BRUKER TENSOR 27 spectrophotometer with KBr pellets from 400 to 4000 cm^{-1}. Elemental analyses (C, H, and N) were carried out on a Flash EA 1112 elemental analyzer. X-ray powder diffraction (XPRD) patterns were recorded using Cu-Kα1 radiation on a PANalytical X'Pert PRO diffractometer. TG measurements were performed by heating the crystalline sample from 20°C to 850°C at 10°C min^{-1} in air on a Netzsch STA 409PC differential thermal analyzer. Fluorescence spectra were performed using a Hitachi 850 fluorescence spectrophotometer at room temperature in solid state. The excitation and emission slit widths are both 2.0 nm.

2.2. *Synthesis of $\{[Zn(bptp)(H_2O)] \cdot 2H_2O \cdot CH_3CN\}_n$ (1)*

A mixture of $ZnCl_2$ (0.0136 g, 0.1 mmol) and H_2bptp (0.0316 g, 0.1 mmol) in 10 mL mixed solvent (CH_3CN/H_2O, V/V, 1:9) was sealed into a 25 mL stainless-steel reactor with a Teflon liner and heated at 170°C for 72 h under autogenous pressure. After the reactor cooled to room temperature at a rate of 5°C h^{-1}, colorless block crystals of **1** suitable for X-ray diffraction were obtained with a yield of 45% (based on Zn). Elemental analysis Calcd for $C_{21}H_{20}N_{10}O_3Zn$ (%): C, 47.96; H, 3.83; N, 26.64. Found (%): C, 48.25; H, 3.52; N, 27.03. IR (cm^{-1}, KBr): 3423s, 3189s, 3079s, 1662w, 1612m, 1578m, 1520m, 1462s, 1423s, 1285m, 1198m, 1104w, 1056m, 1025m, 818 s, 745 s, 645 m.

2.3. *Synthesis of $\{[Pb(bptp)] \cdot H_2O\}_n$ (2)*

The process was similar to **1** except that $ZnCl_2$ was replaced by $Pb(NO_3)_2 \cdot 4H_2O$; light yellow crystals of **2** were obtained with a yield of 60% (based on Pb). Elemental analysis

Table 1. Crystal data and structural refinement of **1** and **2**.

Complex	**1**	**2**
Empirical formula	$C_{21}H_{20}N_{10}O_3Zn$	$C_{19}H_{13}N_9OPb$
Formula weight	525.84	590.57
Temperature (K)	293(2)	293(2)
Wavelength (Å)	0.71073	0.71073
Crystal system	Monoclinic	Monoclinic
Space group	$P2(1)/c$	$C2/c$
Unit cell dimensions (Å, °)		
a	15.511(3)	26.632(5)
b	10.279(2)	9.0982(18)
c	15.780(3)	15.738(3)
α	90	90
β	115.95(3)	100.77(3)
γ	90	90
Volume (Å^3), Z	2262.2(8), 4	3746.3(13), 8
Calculated density (g·cm^{-3})	1.544	2.094
$F(000)$	1080	2224
θ range for data collection (°)	2.45–27.90	2.37–27.90
Reflections collected/unique	15,912/5369	12,952/4443
Data/restraints/parameters	5369/8/326	4443/3/278
Goodness of fit on F^2	1.117	1.065
Final R_1[a], wR_2[b]	0.0709, 0.1785	0.0459, 0.0853

[a]$R_1 = \sum||F_o| - |F_c||/\sum|F_o|$. [b]$wR_2 = [\sum w(|F_o^2| - |F_c^2|)^2/\sum w|F_o^2|^2]^{1/2}$.

Calcd for $C_{19}H_{13}N_9OPb$ (%): C, 38.64; H, 2.22; N, 21.35. Found (%): C, 38.52; H, 2.30; N, 22.14. IR (cm^{-1}, KBr): 3486s, 3369s, 3239m, 3040m, 1658m, 1604m, 1573s, 1515m, 1495m, 1459m, 1420s, 1366m, 1276m, 1181m, 1100m, 1036s, 1023s, 988s, 947w, 818m, 863w, 796m, 744s, 711m, 697m, 644m, 630m.

2.4. *Crystal structure determination*

The data for **1** and **2** were collected on a Rigaku Saturn 724 CCD diffractometer (Mo-Kα, λ = 0.71073 Å) at room temperature. Absorption corrections were applied by using multi-scan program. The data were corrected for Lorentz and polarization effects. The structures were solved by direct methods and refined with a full-matrix least-squares technique based on F^2 with SHELXL-97 crystallographic software package [11]. All non-hydrogen atoms were refined with anisotropic thermal parameters. Hydrogen atoms were located at geometrically calculated positions and refined with isotropic thermal parameters. Crystallographic and refinement details for **1** and **2** are listed in table 1, with selected bond lengths and angles in table 2.

3. Results and discussion

3.1. *H_2bptp and choice of Zn(II) and Pb(II)*

Many helical complexes based on triazole linked bis(pyridine) and pyridine linked bis(azole) ligands were reported by Chen *et al.* and Li *et al.* [12]. H_2bptp consists of

Table 2. Selected bond lengths (Å) and angles (°) for **1** and **2**.

Complex **1**					
Zn(1)–N(4)	2.044(4)	Zn(1)–N(5)	2.121(3)	Zn(1)–O(1 W)	2.051(3)
Zn(1)–N(9)#1	2.146(3)	Zn(1)–N(8)#2	2.151(3)	Zn(1)–N(3)	2.129(3)
N(4)–Zn(1)–O(1W)	177.23(13)	N(4)–Zn(1)–N(5)	77.09(13)	O(1 W)–Zn(1)–N(5)	104.79(13)
N(4)–Zn(1)–N(3)	77.31(13)	O(1 W)–Zn(1)–N(3)	100.84(13)	N(5)–Zn(1)–N(3)	154.36(13)
N(4)–Zn(1)–N(9)#1	89.65(14)	O(1 W)–Zn(1)–N(9)#1	88.41(14)	N(5)–Zn(1)–N(9)#1	87.55(13)
N(3)–Zn(1)–N(9)#1	93.72(13)	N(4)–Zn(1)–N(8)#2	97.30(14)	O(1 W)–Zn(1)–N(8)#2	84.80(14)
N(5)–Zn(1)–N(8)#2	89.37(13)	N(3)–Zn(1)–N(8)#2	92.44(13)	N(9)#1–Zn(1)–N(8)#2	171.59(13)
Complex **2**					
Pb(1)–N(9)#1	2.451(5)	Pb(1)–N(2)	2.565(5)	Pb(1)–N(1)	2.581(5)
Pb(1)–N(6)	2.640(6)	Pb(1)–N(5)#1	2.8070	N(9)#1–Pb(1)–N(2)	78.48(17)
N(9)#1–Pb(1)–N(1)	94.12(17)	N(2)–Pb(1)–N(1)	63.78(17)	N(9)#1–Pb(1)–N(6)	86.49(18)
N(2)–Pb(1)–N(6)	123.01(17)	N(1)–Pb(1)–N(6)	62.96(16)		

Symmetry transformations used to generate equivalent atoms: #1 $-x+1$, $y+1/2$,$-z+1/2$; #2 $-x$, $y-1/2$,$-z+1/2$ for **1**; #1 $-x+1/2$, $y+1/2$,$-z+1/2$ for **2**.

three pyridines linked by two triazole groups and possesses coordination geometry advantages of both triazole linked bis(pyridine) and pyridine linked bis(triazole) ligands. H_2bptp affords more potential coordination sites and has potential to give two bidentate sites, two monodentate ones, and a central tridentate coordination environment.

Two triazoles on the pyridine rings of H_2bptp have a specific bend angle. The resulting frameworks based on H_2bptp must meet the specific angles due to the rigidity of pyridine rings. H_2bptp as a building block is more predictable in the crystal engineering of frameworks than flexible ligands [13]. When H_2bptp is coordinated, it may first use the tridentate chelating site which results in a steric hindrance site. Because of steric hindrance, the pyridyl nitrogen may have a higher priority to coordinate than the remaining triazole nitrogen atoms. To relieve the steric effect, terminal pyridine rings rotate to produce various helical motifs.

Zn(II) and Pb(II) have the ability to form diverse framework structures due to variable coordination geometries with relatively large ionic radii [14]. Pb(II) has a $6s^2$ lone pair in the outer electronic configuration [15] that may provide an opportunity to construct helical complexes.

3.2. *Crystal structure of* $\{[Zn(bptp)(H_2O)]\cdot 2H_2O\cdot CH_3CN\}_n$ *(1)*

Single-crystal X-ray diffraction analysis reveals that the asymmetric unit of **1** consists of one Zn(II), one completely deprotonated $bptp^{2-}$, one coordinated water molecule, two lattice water molecules, and one lattice acetonitrile. As shown in figure 1(a), each Zn(II) lies in a slightly distorted octahedral coordination geometry coordinated by one oxygen (O1W) from coordinated water and five nitrogen atoms (N3, N4, N5, N8A, N9B) from three different $bptp^{2-}$. The Zn–O bond length is 2.051(3) Å and Zn–N bond distances range from 2.044(4) to 2.151(3) Å, all in normal ranges [16]. In **1**, $bptp^{2-}$ adopts the *syn-anti* conformation (scheme 1) and two terminal pyridine rings are twisted by 22.0° with respect to each other. Completely deprotonated $bptp^{2-}$ bridges adjacent Zn(II) centers to form left- and right-handed helical chains viewed along the *c*-axis with a pitch of 10.279 Å (figure 1b). The left- and right-handed helical chains are further linked through sharing common Zn to form a 2-D sheet (figure 1c). Viewing the topology, the

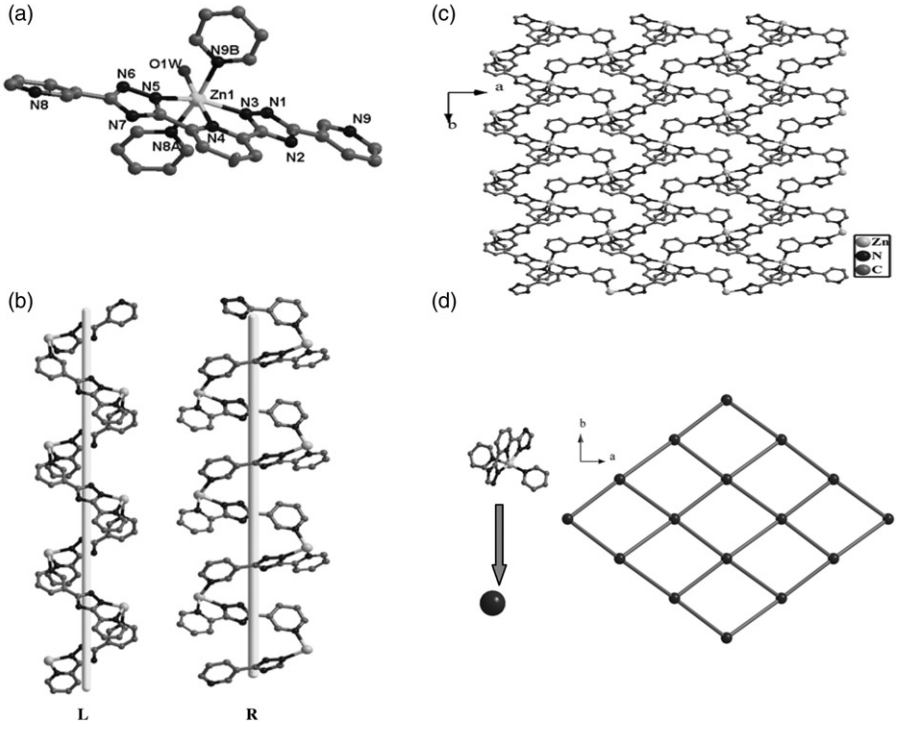

Figure 1. (a) Coordination environment around Zn(II) in **1**, (b) perspective view of the left- and right-handed helices in **1**, (c) the 2-D sheet structure, and (d) schematic representation of the (4,4) net. All hydrogen atoms and coordinated oxygen atoms are omitted for clarity.

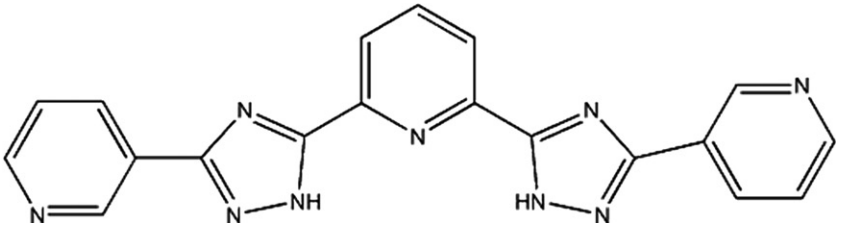

Scheme 1. The *syn-anti* conformation of the ligand in **1**.

2-D layer can be simplified as a (4,4) grid (figure 1d). In most reported helical structures [17], helical chains could be pulled apart without breaking the metal-ion-ligand backbone, while structures with helical chains sharing common metal centers like **1** are rarely reported [18]. Furthermore, adjacent 2-D layers are arranged into a 3-D supramolecular framework by π-π stacking interactions between central pyridine rings and terminal pyridine rings (centroid-to-centroid distance: 3.685 Å).

3.3. *Crystal structure of* $\{[Pb(bptp)]\cdot H_2O\}_n$ *(2)*

Compound **2** exhibits a different 2-D helical network than **1**. The asymmetric unit of **2** consists of one Pb(II), one completely deprotonated $bptp^{2-}$, and one lattice

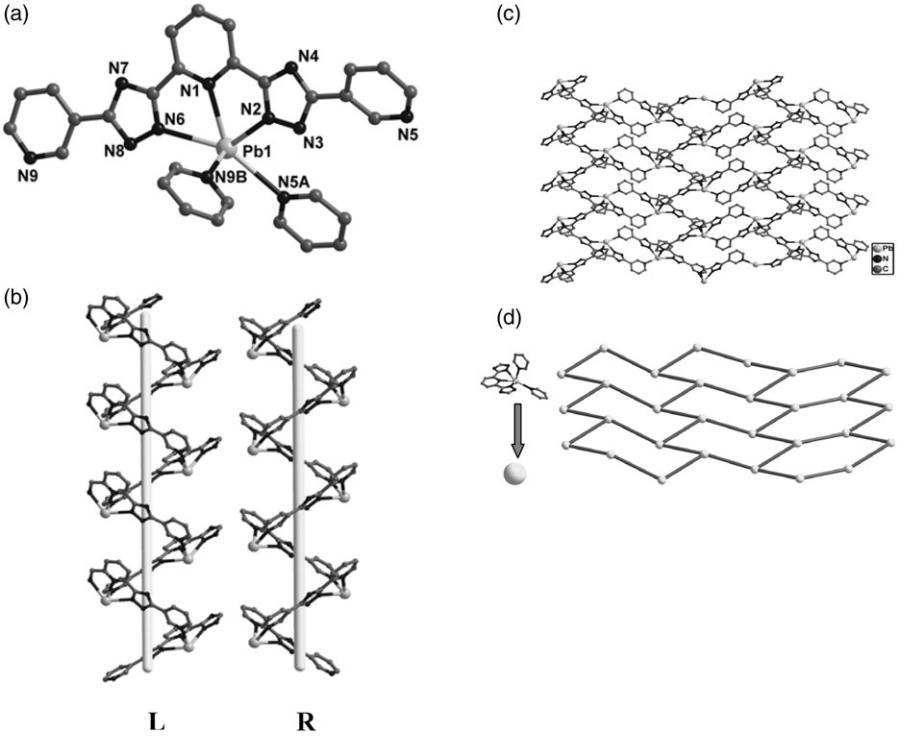

Figure 2. (a) Coordination environment around Pb(II), (b) the right- and left-handed helical chains in the 2-D structure, (c) the 2-D layer structure, and (d) schematic view of the (6,3) topology of **2**. All hydrogen atoms are omitted for clarity.

water molecule. As shown in figure 2(a), each Pb(II) is in a distorted [PbN_5] tetragonal-pyramidal geometry, coordinated by five nitrogen atoms (N1, N2, N6, N5A, N9B) from three different $bptp^{2-}$. The Pb–N bond lengths range from 2.451 Å to 2.807 Å; similar bond lengths are observed in reported complexes [19]. In **2**, completely deprotonated $bptp^{2-}$ adopts the *syn-syn* conformation (scheme 2) and two terminal pyridine rings are twisted by 34.8° with respect to each other. The $bptp^{2-}$ bridges adjacent Pb(II) centers to form the left- and right-handed helical chains viewed along the *b*-axis with identical pitch of 9.098 Å (figure 2b). The left- and right-handed helical chains are further linked through nitrogen from triazole and pyridine to form a 2-D layer (figure 2c). Neighboring helical chains have opposite handedness and **2** shows an overall achiral feature. The 2-D layer can be simplified as a honeycomb-like network with (6,3) topology (figure 2d). The π–π stacking interactions are observed between terminal pyridine rings (N9–C16–C15–C17–C18–C19) and triazole rings (N2–N3–C7–N4–C6), and also between central pyridine rings (N1–C1–C2–C3–C4–C5) and triazole rings (N6–N8–C14–N4–C13), with centroid-to-centroid separation of 3.547 Å and 3.728 Å, respectively, which link adjacent 2-D layers to form a 3-D supramolecular framework.

Complexes **1** and **2** were synthesized under the same reaction conditions except for using different metal salts. H_2bptp adopts distinct conformations in the two complexes, *syn-anti* conformation in **1** and *syn-syn* conformation in **2**. Terminal pyridine ring in

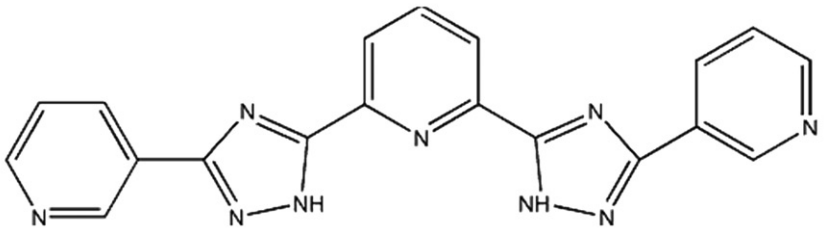

Scheme 2. The *syn-syn* conformation of the ligand in **2**.

$bptp^{2-}$ is twisted by 22.0° in **1** and 34.8° in **2** with respect to the other terminal pyridine ring. This indicates that different conformations can affect the helical features and overall structures of complexes.

3.4. *Comparisons of helices of* 1, 2, *and other helical complexes*

Many helical complexes have been obtained in a "mix-ligand" synthesis system [20], where main ligand or auxiliary ligand bridges metal ions to form helices, and helical chains are further linked through the other ligand to extend to 2-D or 3-D networks [21]. For example, in the helical complex $\{[Zn(L)(phen)(H_2O)]\cdot H_2O\}_n$ (L = 5,6-dihydro-1,4-dithiin-2,3-dicarboxylate), L uses three oxygen atoms of carboxylates to connect two Zn(II), leading to formation of left- and right-handed helical chains [22]. The auxiliary ligand may increase uncertainty of construction of helical structures. However, we choose a long rigid ligand where terminal groups can rotate and take advantage of steric hindrance to directly get complexes with helical motifs. In **1** and **2**, $bptp^{2-}$ both bridge adjacent Zn(II)/Pb(II) centers to form the left- and right-handed helical chains. However, in **1** the left- and right-handed helical chains are alternately connected with Zn(II) acting as hinges to form a 2-D sheet. The structures with helical chains sharing common metal centers like **1** are rare. In **2**, Pb(II) is in a $[PbN_5]$ tetragonal-pyramidal geometry, the left- and right-handed helical chains are further linked through triazole nitrogen atoms and pyridine nitrogen atoms to form a 2-D layer. Because neighboring helical chains have opposite handedness, **2** is overall achiral. Structures with features like **2** are also uncommon.

3.5. *XPRD patterns and thermal analyses*

The XPRD patterns of **1** and **2** are shown in figure S1 and figure S2, respectively. The XPRD patterns determined by experiment are in line with the simulated ones of single crystals, indicating the pure phase of the two compounds. To examine the thermal stability of these complexes, thermal analyses were carried out (figure S3). Both complexes are air-stable and retain their crystalline integrity at ambient temperature. The TGA curve shows weight loss of 14.43% for **1** from 140°C to 200°C corresponding to release of one coordinated water molecule, two free water molecules, and one lattice acetonitrile (Calcd 14.65%) per formula, and then, a plateau region is observed. Residual framework begins to decompose from 460°C. The remaining weight of

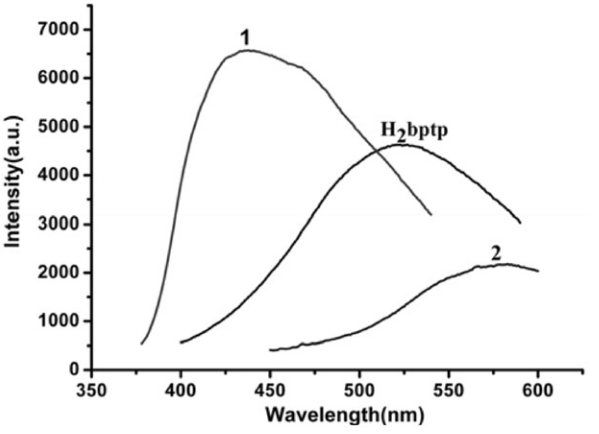

Figure 3. Solid-state emission spectra of **1**, **2**, and free H_2bptp at room temperature.

16.93% corresponds to the percentage of Zn and O components (Calcd 15.48%), indicating that the residue is ZnO. For **2**, a weight loss of 2.94% is detected from 120°C to 250°C corresponding to loss of one free water molecule (Calcd 3.06%) per formula, and then, a plateau region follows. The further weight loss is observed at 500°C due to decomposition of the overall framework. The remaining weight of 38.13% corresponds to the percentage of Pb and O components (Calcd 37.79%), indicating that the residue is PbO. Thermal studies show that **1** and **2** have good thermal stabilities [23].

3.6. *Photoluminescence properties*

Photoluminescence properties of **1** and **2** were investigated in the solid state at room temperature (figure 3). Compound **1** exhibits an intense emission at 438 nm upon excitation at 367 nm, while emission band of **2** appears at 583 nm upon excitation at 415 nm. To understand the emission spectra, luminescence of free H_2bptp under the same experimental conditions was studied for comparison. An intense emission band of H_2bptp is observed at 523 nm upon excitation at 371 nm, assigned to the intraligand $\pi^* \rightarrow \pi$ transition. In comparison with free H_2bptp, the emission peak of **1** is blue-shifted by 95 nm, so the luminescence of **1** may be tentatively assigned to ligand-to-metal charge transfer (LMCT) [24]. The emission peak of **2** is red-shifted by 60 nm relative to H_2bptp, which can be attributed to the mixing of a metal-centered transition involving the s and p metal orbitals and LMCT between delocalized π bonds of $bptp^{2-}$ and p orbitals of Pb(II) [25]. The results indicate that the metal, coordination environment around metal ions and the geometry of ligands play important roles in determining the photoluminescence properties of the complexes.

4. Conclusion

Two new helical complexes have been synthesized with the long N-heterocyclic ligand 2,6-bis(3-(pyrid-3-yl)-1,2,4-triazolyl)pyridine and Zn(II)/Pb(II). Both **1** and **2** possess

2-D networks containing alternating left- and right-handed helical motifs. The ligand in **1** and **2** adopts *syn-anti* and *syn-syn* conformations, respectively. The geometry of the ligand may be one of the most important factors for the construction of the helical structures. Thermal studies reveal thermal stabilities. Complexes **1** and **2** display good luminescent properties at room temperature. That new helical complexes are prepared demonstrates H_2bptp is a suitable candidate for coordination polymers with helical motifs.

Supplementary material

Crystallographic data for the structures reported in this article in the form of CIF files have been deposited with the Cambridge Crystallographic Data Centre, CCDC reference numbers 861 283 and 861 284 for **1** and **2**, respectively. Copies of these data can be obtained free of charge on application to CCDC, 12 Union Road, Cambridge CB2 IEZ, UK (Fax: +44 1 223 336 033; E-mail: deposit@ccdc.cam.ac.uk).

Acknowledgments

This work was financially supported by the National Natural Science Foundation (Nos 20 971 110 and 91 022 013), the Outstanding Talented Persons Foundation of Henan Province.

References

[1] (a) Y. Qi, F. Luo, S. R. Batten, Y.-X. Che, J.-M. Zheng. *Cryst. Growth Des.*, **8**, 2806 (2008); (b) X.-D. Zheng, T.-B. Lu. *CrystEngComm*, **12**, 324 (2010); (c) B. Kesanli, W. Lin. *Coord. Chem. Rev.*, 2**46**, 305 (2003); (d) V. Urban, T. Pretsch, H. Hartl. *Angew. Chem., Int. Ed.*, **44**, 2794 (2005); (e) J.-P. Zhang, Y.-B. Zhang, J.-B. Lin, X.-M. Chen. *Chem. Rev.*, **112**, 1001 (2012).
[2] (a) S.-L. Li, Y.-Q. Lan, J.-S. Qin, J.-F. Ma, J. Liu, J Yang. *Cryst. Growth Des.*, **9**, 4142 (2009); (b) G. Zhang, S.-Y. Yao, D.-W. Guo, Y.Q. Tian. *Cryst. Growth Des.*, **10**, 2355 (2010); (c) B.-L. Wu, L.-Y. Meng, H.-Y. Zhang, H.-W. Hou. *J. Coord. Chem.*, **63**, 3155 (2010); (d) J.-F. Song, R.-S. Zhou, T.-P. Hu, Z. Chen, B.-B. Wang. *J. Coord. Chem.*, **63**, 4201 (2010).
[3] (a) B. Xiao, H. Hou, Y. Fan, M. Tang. *Inorg. Chem. Commun.*, **10**, 376 (2007); (b) X. Li, X. Guo, X.L. Weng, S. Lin. *CrystEngComm*, **14**, 1412 (2012).
[4] (a) C.-P. Li, J.-M. Wu, M. Du. *Inorg. Chem.*, **50**, 9284 (2011); (b) J.-Y. Wu, S.-M. Huang, Y.-C. Huang, K.-L. Lu. *CrystEngComm*, **14**, 1189 (2012); (c) S. Kaizaki, S. Kawata. *Angew. Chem. Int. Ed.*, **45**, 5459 (2006); (d) S.-Z. Zhan, M. Li, J.-Z. Hou, J. Ni, D. Li, X.-C. Huang. *Chem. Eur. J.*, **14**, 8916 (2008).
[5] K. Yoneda, K. Adachi, K. Nishio, M. Yamasaki, A. Fuyuhiro, M. Katada, S. Kaizaki, S. Kawata. *Angew. Chem. Int. Ed.*, **45**, 5459 (2006).
[6] (a) S.-Z. Zhan, D. Li, X.-P. Zhou, X.-H. Zhou. *Inorg. Chem.*, **45**, 9163 (2006); (b) M.-H. Hu, G.-L. Shen, J.-X. Zhang, Y.-G. Yin, D. Li. *Cryst. Growth Des.*, **9**, 4533 (2009).
[7] (a) Y. Wang, B. Ding, P. Cheng, D.-Z. Liao, S.-P. Yan. *Inorg. Chem.*, **46**, 2002 (2007); (b) S. Akine, H. Nagumo, T. Nabeshima. *Inorg. Chem.*, **51**, 5506 (2012); (c) L. Carlucci, G. Ciani, D.M. Proserpio, A. Sironi. *Inorg. Chem.*, **37**, 5941 (1998).
[8] X. Bao, J.-D. Leng, Z.-S. Meng, Z. Lin, M.-L. Tong, M. Nihei, H. Oshio. *Chem. Eur. J.*, **16**, 6169 (2010).
[9] J.-B. Lin, J.-P. Zhang, W.-X. Zhang, W. Xue, D.-X. Xue, X.-M. Chen. *Inorg. Chem.*, **48**, 6652 (2009).
[10] (a) C. Xu, L. Li, Y. Wang, Q. Guo, X. Wang, H. Hou, Y. Fan. *Cryst. Growth Des.*, **10**, 4667 (2011); (b) Z.-H. Zhang, S.-C. Chen, M.-Y. He, C. Li, Q. Chen, M. Du. *Cryst. Growth Des.*, **11**, 5171 (2011).

[11] (a) G.M. Sheldrick. *Acta Cryst*., **A64**, 112 (2008); (b) G.M. Sheldrick. *SHELXS-97, Program for Crystal Structure Solution*, University of Gottingen, Germany (1997).
[12] (a) X.-P. Zhou, D. Li, S.-L. Zheng, X. Zhang, T. Wu. *Inorg. Chem.*, **45**, 7119 (2006); (b) J.-B. Lin, J.-P. Zhang, W.-X. Zhang, W. Xue, D.-X. Xue, X.-M. Chen. *Inorg. Chem.*, **48**, 6652 (2009); (c) F. Cui, S. Li, C. Jia, J.S. Mathieson, L. Cronin, X.-J. Yang, B. Wu. *Inorg. Chem.*, **51**, 179 (2012); (d) A. Williams. *Chem. Eur. J.*, **3**, 15 (1997); (e) L. Cronin, H. Oshio. *Angew. Chem. Int. Ed.*, **50**, 4844 (2011).
[13] Y.-Y. Liu, Y.-Q. Huang, W. Shi, P. Cheng, D.-Z. Liao, S.-P. Yan. *Cryst. Growth Des.*, **7**, 1483 (2007).
[14] (a) J. Yang, J.F. Ma, Y.Y. Liu, J.C. Ma, S.R. Batten. *Inorg. Chem.*, **46**, 6542 (2007); (b) S.R. Fan, L.G. Zhu. *Inorg. Chem.*, **46**, 6785 (2007); (c) Y.H. Zhao, H.B. Xu, Y.M. Fu, K.Z. Shao, S.Y. Yang, Z.M. Su, X.R. Hao, D.X. Zhu, E.B. Wang. *Cryst. Growth Des.*, **8**, 3566 (2008); (d) J. Yang, J.F. Ma, Y.Y. Liu, J.C. Ma, S.R. Batten. *Cryst. Growth Des.*, **9**, 1894 (2009); (e) A.W. Kleij, M. Kuil, D.M. Tooke, A.L. Spek, J.N.H. Reek. *Inorg. Chem.*, **44**, 7696 (2005); (f) T.M. McCormick, S. Wang. *Inorg. Chem.*, **47**, 10017 (2008).
[15] (a) S.H. Deo, A. Godwin. *J. Am. Chem. Soc.*, **122**, 174 (2000); (b) J. Li, Y. Lu. *J. Am. Chem. Soc.*, **122**, 10466 (2000); (c) M.H. Jack, M. Saeed, A.S. Ali. *Inorg. Chem.*, **43**, 1810 (2004); (d) L.K. Li, Y.L. Song, H.W. Hou, Y.T. Fan, Y. Zhu. *Eur. J. Inorg. Chem.*, 3238 (2005).
[16] (a) L. Yi, L.-N. Zhu, B. Ding, P. Cheng, D.-Z. Liao, S.-P. Yan, Z.-H. Jiang. *Inorg. Chem. Commun.*, **6**, 1209 (2003); (b) R.T. Stibrany, J. Vasudevan, S. Knapp, J.A. Potenza, T. Emge, H.J. Schugar. *J. Am. Chem. Soc.*, **118**, 3980 (1996); (c) X.-C. Huang, Y.-Y. Lin, J.-P. Zhang, X.-M. Chen. *Angew. Chem. Int. Ed.*, **45**, 1557 (2006).
[17] (a) H. Bai, K. Xu, Y. Xu, H. Matsui. *Angew. Chem. Int. Ed.*, **46**, 3319 (2007); (b) R. Wang, Y. Zhou, Y. Sun, D. Yuan, L. Han, B. Lou, B. Wu, M. Hong. *Cryst. Growth Des.*, **5**, 251 (2005); (c) Y.-F. Guan, Z.-Y. Li, M.-F. Ni, C. Lin, J. Jiang, Y.-Z. Li, L. Wang. *Cryst. Growth Des.*, **11**, 2684 (2011); (d) W.-G. Lu, J.-Z. Gu, L. Jiang, M.-Y. Tan, T.-B. Lu. *Cryst. Growth Des.*, **8**, 192 (2008).
[18] (a) L. Yi, X. Yang, T. Lu, P. Cheng. *Cryst. Growth Des.*, **5**, 1215 (2005); (b) E. Yashima, K. Maeda, H. Iida, Y. Furusho, K. Nagai. *Chem. Rev.*, **109**, 6102 (2009); (c) C. Piguet, G. Bernardinelli, G. Hopfgartner. *Chem. Rev.*, **97**, 2005 (1997).
[19] (a) F. Marandi, B. Mirtamizdoust, A.A. Soudi, H-K. Fun. *Inorg. Chem. Commun.*, **10**, 174 (2007); (b) Q.-Y. Li, F. Zhou, C. Zhai, L. Shen, X.-Y Tang, J. Yang, G.-W. Yang, Z.-F. Miao, J.-N. Jin, W. Shen. *Inorg. Chem. Commun.*, **14**, 843 (2011); (c) W.A. Merrill, R.J. Wright, C.S. Stanciu, M.M. Olmstead, J.C. Fettinger, P.P. Power. *Inorg. Chem.*, **49**, 7097 (2010).
[20] (a) H.-J. Hao, C.-W. Lin, X.-H. Yin, F. Zhang. *J. Coord. Chem.*, **64**, 965 (2011); (b) A. Panja. *J. Coord. Chem.*, **64**, 987 (2011); (c) T.-J. Won, J.K. Clegg, L.F. Lindoy, J.C. McMurtrie. *Cryst. Growth Des.*, **7**, 972 (2007); (d) W.-G. Lu, J.-Z. Gu, L. Jiang, M.-Y. Tan, T.-B. Lu. *Cryst. Growth Des.*, **8**, 192 (2008).
[21] (a) X. Wang, Y. Liu, C. Xu, Q. Guo, H. Hou, Y. Fan. *Cryst. Growth Des.*, **12**, 2435 (2012); (b) L. Han, Y. Zhou, W.-N. Zhao, X. Li, Y.-X. Liang. *Cryst. Growth Des.*, **9**, 660 (2009); (c) R. Wang, Y. Zhou, Y. Sun, D. Yuan, L. Han, B. Lou, B. Wu, M. Hong. *Cryst. Growth Des.*, **5**, 251 (2005).
[22] S-M. Fang, D.-L. Peng, M. Chen, L.-R. Jia, M. Hu. *J. Coord. Chem.*, **65**, 668 (2012).
[23] (a) Z.-G. Gu, Y.-T. Liu, X.-J. Hong, Q.-G. Zhan, Z.-P. Zheng, S.-R. Zheng, W.-S. Li, S.-J. Hu, Y.-P. Cai. *Cryst. Growth Des.*, **12**, 2178 (2012); (b) T. Jia, S. Zhu, M. Shao, Y. Zhao, M. Li. *Inorg. Chem. Commun.*, **11**, 1221 (2008); (c) S.-Q. Zhang, F.-L. Jiang, M.-Y. Wu, R. Feng, J. Ma, W.-T. Xu, M.-C. Hong. *Inorg. Chem. Commun.*, **14**, 1400 (2011); (d) R. Hu, H. Cai, J. Luo. *Inorg. Chem. Commun.*, **14**, 433 (2011).
[24] (a) L. Hou, D. Li. *Inorg. Chem. Commun.*, **8**, 190 (2005); (b) J. Tao, J.-X. Shi, M.-L. Tong, X.-X. Zhang, X.-M. Chen. *Inorg. Chem.*, **40**, 6328 (2001).
[25] (a) G.-B. Che, J. Chen, X.-C. Wang, C.-B. Liu, C.-J. Wang, S.-T. Wang, Y.-S. Yan. *Inorg. Chem. Commun.*, **14**, 1086 (2011); (b) A. Vogler, A. Paukner, H. Kunkely. *Coord. Chem. Rev.*, **33**, 227 (1980); (c) P.C. Ford, A. Vogler. *Acc. Chem. Res.*, **26**, 220 (1993); (d) B. Ding, Y.Y. Liu, X.X. Wu, X.-J. Zhao, G.X. Du, E.-C. Yang, X.G. Wang. *Cryst. Growth Des.*, **9**, 4176 (2009); (e) L. Zhang, Z.-J. Li, Q.-P. Lin, Y.-Y. Qin, J. Zhang, P.-X. Yin, J.-K. Cheng, Y.-G. Yao. *Inorg. Chem.*, **48**, 6517 (2009); (f) Z. Chen, J. Yan, H. Xing, Z. Zhang, F. Liang. *J. Solid State Chem.*, **184**, 1063 (2011).